

Entanglement Fractalization

Yao Zhou and Peng Ye*

School of Physics, State Key Laboratory of Optoelectronic Materials and Technologies, and Guangdong Provincial Key Laboratory of Magnetoelectric Physics and Devices, Sun Yat-sen University, Guangzhou, 510275, China
(Dated: Friday 3rd November, 2023)

We investigate the quantum entanglement of free-fermion models on fractal lattices with non-integer dimension and broken translation symmetry. For gapless systems with finite density-of-state at the chemical potential, we find a universal scaling of entanglement entropy (EE) as $S_A \sim L_A^{d_s-1} \log L_A$ that is independent of the partition scheme, where d_s is the space dimension where fractals are embedded, and L_A is the linear size of the subsystem A . This scaling extends the Widom conjecture of translation-invariant systems to fractal lattices. We also study entanglement contour (EC) as a real-space entanglement “tomography”. The EC data show a self-similar and universal pattern called “entanglement fractal” (EF), which resembles Chinese papercutting and keeps invariant for different partition schemes, leading to the EE scaling robustness. We propose a set of rules to artificially generate the EF pattern, which matches the numerical results at the scaling limit. For gapped systems, we observe that the fractal feature of A ’s boundary affects the EE scaling as $S_A \sim L_A^{d_{bf}}$, where d_{bf} is the Hausdorff dimension of A ’s boundary, generalizing the area law. Meanwhile, the EC mainly localizes at A ’s boundary. Our study reveals how fractal geometry interacts with the entanglement of free fermions. Future directions from physics and mathematics are discussed, e.g., experimental verification and Laplacian on fractals.

Introduction— Entanglement offers a quantum-informative perspective to understand the non-local correlation in many-body quantum systems [1–3]. The entanglement entropy (EE) of gapped ground states follows a universal scaling feature called area law [2–4]. Topological entanglement entropy is a direct measure for total quantum dimension of anyon models, i.e., 2D topological order [5, 6]. The entanglement spectra of gapped topological systems encode their universal properties of topological edge states [7–9]. For gapless systems with codimension-1 Fermi surface, the EE scales as “super area law” $S \sim L^{d_s-1} \log L$ associated with the celebrated Widom conjecture for translation-invariant systems [3, 10–15], where $d_s = 1, 2, 3, \dots$ is the spatial dimension.

However, the dimension is not always an integer. One can also place either local qubits or quantum particles on fractal lattices whose Hausdorff dimension can be non-integer [16]. In fact, fractals are not rare but common in nature. Academically, since the last century, statistical models and critical phenomena on fractals have attracted great research interest [17–23]. Till now, efforts have been continuously made and many interesting physical phenomena have been explored [24–36], such as topological effects, optical and transport properties, and practical implementation of fractal topological quantum memory, etc. It has been clear that all the above findings substantially depend on the unique features of fractals: fractional dimension felt by microscopic degrees of freedom and self-similarity with broken translation symmetry.

While the EE of translation-invariant systems relies on the Widom conjecture of Toeplitz matrices, it is thus natural to ask whether there exists a generalized Widom conjecture for the asymptotic behaviors of the matrices with self-similarity to determine the EE of quantum many-body systems on fractal lattices that lack translation symmetry and provide a non-integer dimension. Alternatively speaking, it is important to

explore the interplay of quantum entanglement and fractal geometry, which motivates this work.

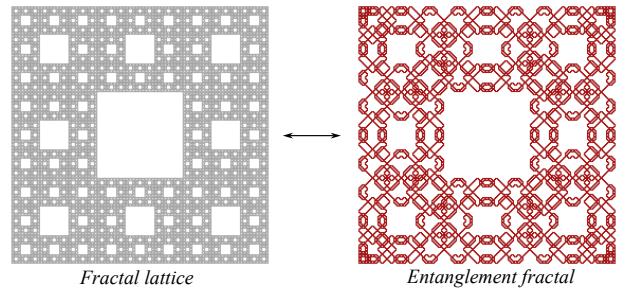


FIG. 1. Pictorial illustration of fractal lattice and entanglement fractal which resembles Chinese papercutting. See main texts for details.

In this work, we consider free-fermion systems defined on Sierpinski carpets and study entanglement properties, including the EE mentioned above and the entanglement contour (EC) [37] that is a real-space “tomography” of quantum entanglement. Specifically, we first consider a gapless system whose fractal lattice is embedded in 2D space and has a finite density-of-state (DOS) at the chemical potential. To measure the entanglement between complementary regions of a pure state, we partition the fractal lattice into two parts A and B using various partition schemes, in which A ’s boundary may be either regular 1D curves or fractal curves (e.g., Cantor set). We find a universal scaling of EE for generic free-fermion systems on fractal lattices with a finite DOS at the chemical potential: $S_A = aL_A^{d_s-1} \log L_A + \dots$, where a is a nonuniversal constant. Here, d_s is the dimension of the embedding space and $d_s = 2$ for our numerical setting. L_A is the linear size of the subsystem A . This scaling extends the traditional Widom conjecture for translation-invariant systems to fractal lattices. To further understand the EE result and look for the entanglement fingerprint of the Hausdorff dimension of the original lattice, we study the EC, which exhibits a self-similar and universal pattern called “entanglement fractal” (EF). The EF

* yepeng5@mail.sysu.edu.cn

pattern resembles Chinese papercutting (Fig. 1) and is invariant for different partition schemes, which leads to the robustness of the EE scaling. To understand general properties of the EF pattern, we propose a set of rules and artificially generate the EF pattern, which matches the numerical results. For gapped systems, from the numerical analysis, we propose a universal scaling of EE as $S_A = aL_A^{d_{\text{bf}}} + \dots$ where d_{bf} is the Hausdorff dimension of A 's boundary, which generalizes the conventional area law. Moreover, as a common feature of gapped systems, the EC mainly distributed at A 's boundary and exponentially decay into bulk.

Preliminaries— We begin by giving a brief introduction to the entanglement characterization of many-body ground states in fractal systems. Consider a many-body ground state $|G\rangle$ with density matrix $\rho = |G\rangle\langle G|$. If we partition the fractal system into two subsystems A and B , we can obtain the reduced density matrix $\rho_A = \text{Tr}_B |G\rangle\langle G| = \frac{1}{N} \exp(-\mathcal{H}^E)$ by tracing over the subsystem B , where N is a normalization constant. In the free-fermion limit, the EE S_A can be calculated from the equation $S_A = \text{Tr}(f(C^A)) = \sum_i f(\xi_i)$ with $f(x) = -[x \log x + (1-x) \log(1-x)]$ [38, 39], where the spectrum $\{\xi_i\}$ is the correlation matrix of the subsystem A defined as $C^A(i, j) = \langle G | c_i^\dagger c_j | G \rangle$ with $i, j \in A$. Before we focus on studying the entanglement features of fractal systems, we need to consider the process of constructing a lattice system with a fractal structure. First, we introduce an initial unit cell and a fractal iteration method, which are two variable elements of the fractal lattice and uniquely determine a kind of fractal lattice. By applying the iteration method acting on the unit cell repeatedly n times, we can obtain the n th-order approximation of the fractal, such as the 5th-order approximation $SC(5, 1)$ of Sierpinski carpet [16] as shown on the left of Fig. 1 (see Supplemental Materials (SM)-A for more details).

EE of gapless systems on the fractal lattice— Here we study the scaling of EE for the gapless system defined on the fractal lattice $SC(n, 1)$ embedded in 2-dimensional spatial space as shown in Fig. 2(a). We consider a spinless tight-binding model given by $H_1 = -t \sum_{\langle ij \rangle} c_i^\dagger c_j - \mu \sum_i c_i^\dagger c_i$, where c_i^\dagger is a fermionic creation operator at the i th lattice site, $\langle ij \rangle$ denotes nearest-neighbor sites, and μ is chemical potential. This model H_1 has some symmetries due to the properties of the fractal lattice $SC(3, 1)$, such as a four-fold rotation symmetry. To determine the bulk gap, we need to calculate the energy spectrum of the model H_1 on the fractal lattice $SC(n, 1)$. Since the number of lattice sites exponentially increases upon the iterated generation of the fractal lattice [16], the numerical exploration of entanglement poses substantial challenges. More concretely, numerical calculation in entanglement of translation-invariant systems relies on diagonalization of a non-sparse matrix at large size limit, the challenge now is substantially enhanced as translation symmetry is further lacking, which calls for comparably computationally cost numerical study. Back to our case, through analyzing the scaling of the energy gap and the density of states, we show that the model H_1 on the Sierpinski carpet has a gapless ground state. The technical details are given in SM-B.

We first discuss different partition schemes. Fig. 2(a) shows

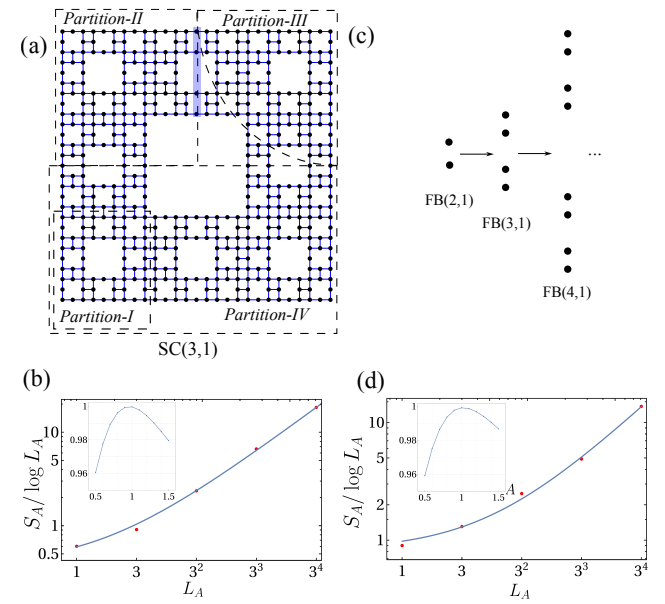


FIG. 2. (a) Four kinds of partitions on the 3rd-order approximation $SC(3, 1)$ of Sierpinski carpet as an example. Partition-I has a normal boundary and Partition-II has a fractal boundary in the blue area. (c) The fractal structure of the boundary in the blue area in (a) for different n . (b) and (d) The EE of the model on the n th-order approximation $SC(n, 1)$ of Sierpinski carpet, using Partition-I and Partition-II, respectively. The insets show the coefficient of determination R^2 as a function of α to measure the goodness of fit. Here $t = 1$ and $\mu = 0$.

the 3rd-order approximation $SC(3, 1)$ of Sierpinski carpet as an example, where we illustrate four kinds of partitions (I-IV). For Partition-I, we divide $SC(3, 1)$ into two subsystems A and B , where A is the 2nd-order approximation $SC(2, 1)$ that preserves the all spatial symmetry of the original lattice. In general, for the n th-order approximation $SC(n, 1)$, A is the $(n-1)$ th-order approximation $SC(n-1, 1)$ with the linear length $L_A = 3^{n-1}l$ and the number of the boundary sites $N_{bA} = 3^{n-1}$, where the lattice constant $l = 1$. Then, since $L_A = N_{bA}$, A 's boundary by using Partition-I in Fig. 2(a) is a regular 1D line.

Next, we use Partition-I to study the EE scaling for the model H_1 on $SC(n, 1)$. As discussed in SM-B, the energy gap of the model H_1 on Sierpinski carpet vanishes at scaling limit and the DOS is finite, indicating a gapless nature. It is known that, the model H_1 on a square lattice admits a one-dimensional Fermi surface with finite DOS, and its EE scales as $S_A = aL_A \log L_A + \dots$, where the coefficient a is determined by the detail of Fermi surface and partition scheme and can be calculated from the Widom conjecture [13]. Therefore, we propose that the EE when the model is placed on the Sierpinski carpet would also scale as $S_A = aL_A^\alpha \log L_A + \dots$, where the parameter α might encode the fractal information of the lattice, and a is still a nonuniversal constant. To support this proposal, we numerically obtain S_A for different n of $SC(n, 1)$ to enlarge the fractal lattice size, as shown in Fig. 2(b). By fitting the numerical data with $\alpha = 1$, we get

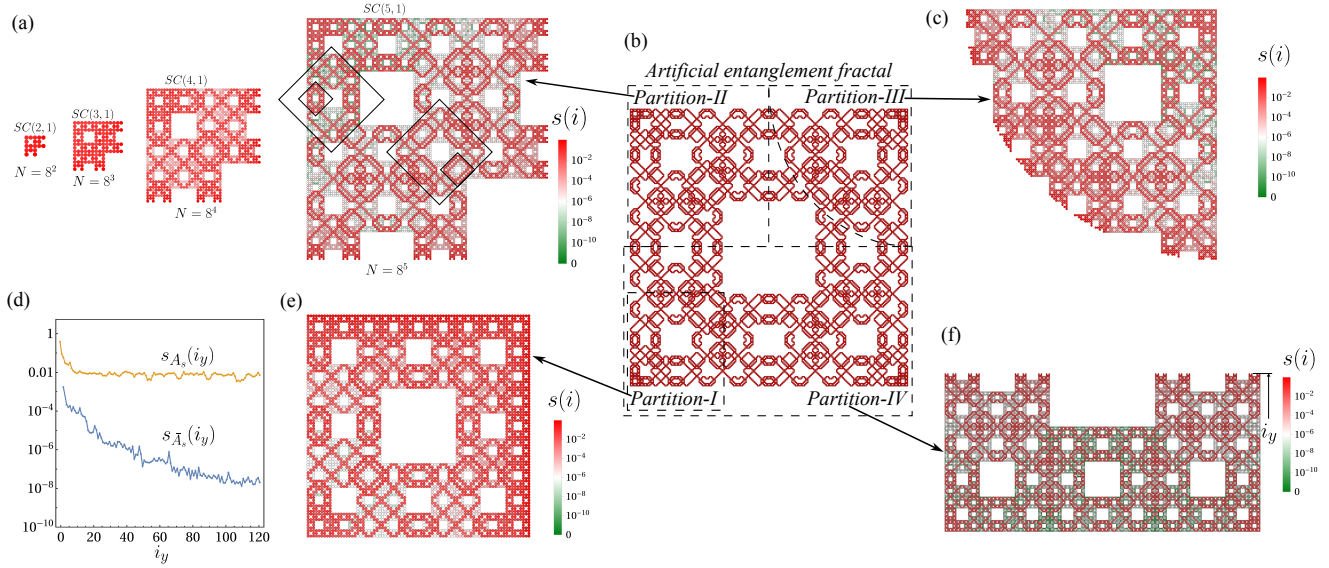


FIG. 3. (a) Entanglement contour (EC) of the model H_1 on the n th-order approximation $SC(n, 1)$ using Partition-II. (b) The artificially generated structure, called *entanglement fractal* (EF), and its four partitions. (c), (e) and (f) are EC of the model H_1 using Partition-I, Partition-III and Partition-IV, respectively. The dominant EC of (a), (c), (e), and (f) matches the artificially generated EF pattern in (b). (d) The behavior of EC s_i on the self-similar structure A_s and the rest of the subsystem A , where the yellow and blue lines represent $s_{A_s}(i_y)$ and $s_{\bar{A}_s}(i_y)$, respectively.

$S_A / \log L_A = 0.37143 + 0.22372 L_A$. Moreover, we use the coefficient of determination R^2 as a function of α to measure the goodness of fit, as shown in the inset of Fig. 2(b). We find that $\alpha \approx 1$ is the best fit with R^2 closest to 1. Based on this fitting expression in 2D where the fractal lattice is embedded, we propose that the EE scaling of the model H_1 on the fractal lattice is

$$S_A = a L_A^{d_s-1} \log L_A + \dots, \quad (1)$$

where d_s is the spatial dimension. This expression is the same as that of gapless systems with codimension-1 Fermi surface in translation-invariant systems despite the obviously different nonuniversal constant a .

In addition to Partition-I, we adopt Partition-II in Fig. 2(a) to test Eq. (1). In this case, A explicitly breaks the symmetry and fractal structure of Sierpinski carpet. We find that the linear length of A 's boundary is $L_A = 3^{n-1}l$ in $SC(n, 1)$ and the number of sites on the boundary is $N_{bA} = 2^{n-1}$, as shown in Fig. 2(c) for different n . Since $L_A > N_{bA}$, the boundary “ $FB(n, 1)$ ” of A supports a fractal structure. We define a boundary Hausdorff dimension $d_{bf} = \log_{L_A} N_{bA} = \log_3 2$ for $FB(n, 1)$, which can be seen as the n th-order approximation of Cantor set [16]. With this preparation, we numerically obtain the EE on $SC(n, 1)$ as shown in Fig. 2(d). We expect that the EE scaling in this case is still $S_A = a L_A^\alpha \log L_A + \dots$. By fitting the data with $\alpha = 1$, we get $S_A / \log L_A = 0.82249 + 0.15858 L_A$. The best fit is $\alpha \approx 1$ with the coefficient of determination R^2 closest to 1, as shown in the inset of Fig. 2(d). Based on these results, the EE scaling of the model H_1 on the fractal lattice is still given by Eq. (1). While it is practically impossible to exhaust infinite kinds of partition schemes, the above two partitions, i.e.,

Partition-I and Partition-II, which respectively preserve and break the symmetry the original Sierpinski carpet, are representative cases. Thus, we conclude that Eq. (1) is the universal scaling of EE of gapless free-fermion systems with finite DOS on fractal lattice that is embedded in d_s dimensional space.

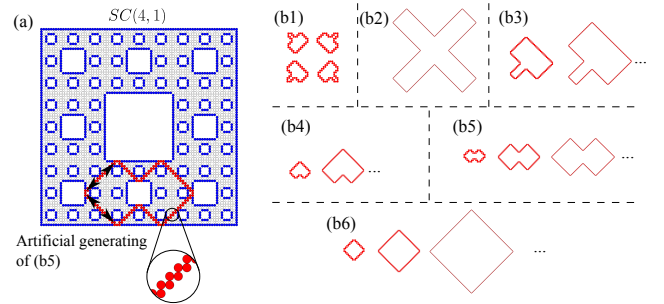


FIG. 4. (a) Illustration of the artificial generating rules for *entanglement fractal* on the 4th-order approximation $SC(4, 1)$. The red closed loop shows the artificial generating structure of (b5) in the gapless fractal systems and the blue sites are the boundaries of $SC(4, 1)$. (b1-b6) All possible structures by the artificial generating rules.

Entanglement fractals and its artificially generating— To further explore entanglement fingerprint of fractal geometry and fine structure of EE, we study an entanglement quantity called entanglement contour (EC) [37], which gives rise to a real-space “tomography” of EE. The EC in free-fermion systems is defined as $s(i) = \sum_\ell p_i(\ell) S_\ell$, where $S_\ell = -[\xi_\ell \log \xi_\ell + (1 - \xi_\ell) \log(1 - \xi_\ell)]$. $p_i(\ell) = |\langle i | \ell | i \rangle|^2$ is the probability of the eigenvector $|\ell\rangle$ of the correlation matrix at

the site i in A , and $\sum_i p_i(\iota) = 1$. The eigenvectors $|\iota\rangle$, often called ‘‘Schmidt vectors’’ or ‘‘entanglement wavefunctions’’, include the information of bulk-boundary correspondence in topological gapless systems [40]. By using EC, we can reconstruct EE as $S_A = \sum_i s(i)$. We first use Partition-II to examine the distribution of EC $s(i)$ of the model H_1 on $SC(n, 1)$. As shown in Fig. 3(a), we numerically find that when the system size increases, the dominant $s(i)$ exhibits more and more clear patterns in the bulk of A , which resembles Chinese paper cutting. Moreover, we find that the EC has self-similarity, as shown in the black rhombus of the rightmost subfigure [i.e., $SC(5, 1)$] of Fig. 3(a), which is a part of the EF pattern distributed in the whole space. We will introduce EF shortly. To proceed further, we use Partition-I, III and IV to examine EC of the model H_1 on $SC(5, 1)$. All numerical results are given in Fig. 3(a), (c), (e) and (f), where dominant EC data have a clear self-similar structure.

To understand the numerical results, we summarize a set of generating rules in order to artificially generate dominant EC on the fractal lattice $SC(n, 1)$ shown in Fig. 3 (a), (c), (e) and (f). As an example, we plot a red closed loop in $SC(4, 1)$ in Fig. 4(a), where the blue sites constitute the boundaries of $SC(4, 1)$. The basic rules include:

- The dominant EC is formed by closed loops;
- Each loop line starts from and undergoes specular reflection at the boundaries of $SC(n, 1)$;
- Each loop line extends along the directions of 45° , 135° , 225° and 315° with two sites as shown by the arrows in Fig. 4(a).

Following these rules, we artificially generate all possible structures on the fractal lattice $SC(n, 1)$ as shown in Fig. 4(b1-b6). We find that the patterns in Fig. 4(b3-b6) are self-similar, while the pattern set in Fig. 4(b3) does not appear in EC of H_1 on $SC(n, 1)$. The forbidden EC may depend on the fractal structure or the Hamiltonian model (see SM-C for more details). By applying the patterns in Fig. 4(b1-b2) and (b4-b6) on $SC(5, 1)$, we successfully generate a fractal structure on $SC(5, 1)$, as shown in Fig. 3(b). Next, by applying Partition-(I-IV) to Fig. 3(b) and comparing the resulting patterns with the numerical results in Fig. 3(a), (c), (e) and (f), we find that the distribution of dominant EC data in the bulk of A , are almost identical to the artificially generated pattern shown in Fig. 3(b). We call this discernible EC structure *entanglement fractal* (EF), which can be seen as the entanglement fingerprint of fractal geometry. We also infer that the universal scaling of the EE originates from the above EF pattern.

Next, we observe different behaviors of $s(i)$ on EF and the rest of the subsystem A , as shown in Fig. 3(f). To quantify $s(i)$ on different areas, we define a quantity:

$$s_{A_s(\bar{A}_s)}(i_y) = \sum_{i_x \in A_s(\bar{A}_s)} s(i_x, i_y) / \left(\sum_{i_x \in A_s(\bar{A}_s)} 1 \right) \quad (2)$$

to measure the behavior of $s(i)$, where A_s and \bar{A}_s represent EF and the rest of A , respectively, and i_y is the distance from A ’s boundary. As shown in Fig. 3(d), $s_{A_s}(i_y)$ displays a

power-law decay with increasing i_y , while $s_{\bar{A}_s}(i_y)$ shows an exponential decay. Based on EF and the behavior of $s(i)$ in A , we propose an equation for calculating the EE of the gapless system on the fractal lattice as

$$S_A = \sum_{i \in A_s} s(i) + \dots \quad (3)$$

Here the ellipsis represents the subleading term $\sum_{i \in \bar{A}_s} s(i)$ of the EE. Compared to the expression of EE $S_A = \text{Tr}[f(C^A)]$ [38, 39] in free-fermion systems, Eq. (3) provides information about the asymptotic behavior for the spectrum of the correlation matrix C^A , which may help us analytically generalize the Widom conjecture of Toeplitz matrices to the matrices with self-similarity. Mathematically, the Brownian motion on the infinitely ramified self-similar fractals (see Refs. [41, 42] and references therein), such as Sierpinski carpet, is a notorious problem, which is associated with the asymptotic behaviors of Laplacian on the fractals [43, 44]. Once we obtain a new ‘conjecture’ for the asymptotic behaviors of the matrices with self-similarity is helpful for understanding the Brownian motion on fractals, which is an important direction for future study.

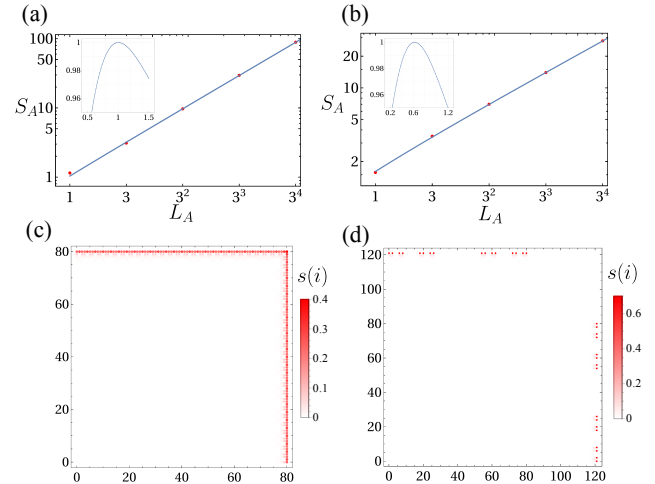


FIG. 5. (a) and (b) are the EE of the model H_2 as a function of the number of iteration n by using Partition-I and II, respectively. The insets show the coefficient of determination R^2 as a function of α to measure the goodness of fit. (c) and (d) are the distribution of EC of the model H_2 in the subsystem A of $SC(5, 1)$ by using Partition-I and II, respectively. Here $t_1 = 0.5$ and $t = 1$.

Entanglement of gapped systems on fractal lattice— Turning to the entanglement of gapped systems on fractals, we consider a tight-binding model on the fractal lattice $SC(n, 1)$ embedded in a two-dimensional space, as shown in Fig. 2(a). The model is given by $H_2 = \sum_i (c_{s,i}^\dagger c_{p,i}^\dagger) t_1 \sigma_x (c_{s,i} c_{p,i})^T + \sum_{i,j} (c_{s,i}^\dagger c_{p,j}^\dagger) t \sigma_z (c_{s,i} c_{p,j})^T$, where $c_{s(p),i}^\dagger$ is a fermionic creation operator of $s(p)$ orbital at the i th lattice site and $\sigma_{x,y}$ are Pauli matrices. As discussed in SM-B, through analyzing the scaling of the energy gap and the density of states, we find that the ground state of the model is gapped.

Due to the existence of a finite gap, we propose that the EE of this model H_2 on the Sierpinski carpet would scale as $S_A = aL_A^\alpha + \dots$, where α is a universal parameter to be determined. To verify this proposal, we first adopt Partition-I in Fig. 2(a) to study the scaling of EE of the model H_2 on the n th-order approximation $SC(n, 1)$ of Sierpinski carpet. As shown in Fig. 5(a), by fitting the data with $\alpha = 1$, the numerical data of EE is fit to $S_A = 1.10033L_A - 0.120981$. The best fit is $\alpha \approx 1$ with the coefficient of determination R^2 closest to 1, as shown in the inset of Fig. 5(a). Furthermore, we consider Partition-II in Fig. 2(a) to divide $SC(n, 1)$ into A and B , where the boundary $FB(n, 1)$ in the blue area of Fig. 2(a) has fractal structure. Through numerical calculation, the EE of the model H_2 in this case is demonstrated in Fig. 5(b). By fitting the numerical data, the EE scales to $S_A = 1.84893L_A^{0.62} - 0.234274$, where $\alpha \approx 0.62$ is the best fit with the coefficient of determination R^2 closest to 1. Note that for Sierpinski carpet, its spatial dimension $d_s = 2$ and Hausdorff dimension $d_f = \log_3 8 \approx 1.8928$, while the boundary $FB(n-1)$ of the subsystem A has the Hausdorff dimension $d_{bf} = \log_3 2 \approx 0.6309$. Combining the numerical results of EE with Partition-I and II, we observe that the EE of the gapped systems only reflects the fractal feature of the subsystem's boundaries. Then, for gapped systems on fractal, we obtain a generalized area law written as

$$S_A = aL_A^{d_{bf}} + \dots, \quad (4)$$

where d_{bf} is the boundary Hausdorff dimension. Finally, considering the EC $s(i)$ in this case, as demonstrated in Fig. 5(c) and (d), the distribution of $s(i)$ is localized at the boundaries of the subsystem A .

Discussions— In this work, we have studied the interplay of fractal geometry and quantum entanglement of free fermions through two entanglement quantities: entanglement entropy (EE) and entanglement contour (EC). Several interesting problems arise and call for future study. For example, we have proposed several rules to artificially generate the entanglement fractals (EF) in Fig. 3(b) that are formed by the dominant EC data at the scaling limit. However, the underlying theory of EF is yet to be constructed, which is the next important step towards understanding the generalized Widom

conjecture on fractals that break translation symmetry and have non-integer dimensions. To find the theory, we adopt alternative way, which fractally adjusts the hopping term of the tight-binding model on normal lattice, to diagnose the EE and EC, while we propose that the topology of Fermi surface [45] may affect the structure of the EF. Meanwhile, when conventional orders such as superconducting order are established on fractals with finite DOS at the chemical potential, it is interesting to investigate the variation of EF. Furthermore, motivated by the Widom conjecture for Toeplitz matrices in translation-invariant systems when calculating EE, it is important to study the asymptotic behavior of correlation matrix on fractals, which immediately helps us to determine the analytic form of the non-universal coefficient a in the EE scaling formulas. Generally, the correlation matrix inherits symmetries from the Hamiltonian of lattice systems, such as the translation invariance and self-similarity, etc. Then, through exploring the conjecture about the asymptotic behavior of the correlation matrix on fractals, we gain valuable insights into the asymptotic behavior of a specific class of matrices with self-similarity. Meanwhile, such an effort offers a pathway for diagnosing the Brownian motion on fractals, connecting it with the spectral behaviors of the Laplacian on fractals [43, 44]. From the numerical perspective, even for the free-fermion system on fractal, the efficient numerical method also needs to be investigated to extract the information of entanglement.

With the progress of experimental techniques, the lattice system with fractal structure can be realized experimentally in physics and chemistry [24–28], which paves a way for studying the many-body systems with fractal geometry. Moreover, in phononic platform, it is possible to simulate and measure the entanglement of many-body systems from the pumping-probe responses in fractal phononic lattice [35, 46].

Acknowledgments— This work was supported by NSFC Grant No. 12074438, Guangdong Basic and Applied Basic Research Foundation under Grant No. 2020B1515120100, the Open Project of Guangdong Provincial Key Laboratory of Magnetoelectric Physics and Devices under Grant No. 2022B1212010008, and Fundamental Research Funds for the Central Universities, Sun Yat-sen University (No. 23ptpy05).

[1] Luigi Amico, Rosario Fazio, Andreas Osterloh, and Vlatko Vedral, “Entanglement in many-body systems,” *Rev. Mod. Phys.* **80**, 517–576 (2008).

[2] J. Eisert, M. Cramer, and M. B. Plenio, “Colloquium: Area laws for the entanglement entropy,” *Rev. Mod. Phys.* **82**, 277–306 (2010).

[3] Nicolas Laflorencie, “Quantum entanglement in condensed matter systems,” *Physics Reports Quantum Entanglement in Condensed Matter Systems*, **646**, 1–59 (2016).

[4] M. B. Hastings, “An area law for one-dimensional quantum systems,” *J. Stat. Mech.* **2007**, P08024 (2007).

[5] Alexei Kitaev and John Preskill, “Topological entanglement entropy,” *Phys. Rev. Lett.* **96**, 110404 (2006).

[6] Michael Levin and Xiao-Gang Wen, “Detecting topological order in a ground state wave function,” *Phys. Rev. Lett.* **96**, 110405 (2006).

[7] Hui Li and F. D. M. Haldane, “Entanglement spectrum as a generalization of entanglement entropy: Identification of topological order in non-abelian fractional quantum hall effect states,” *Phys. Rev. Lett.* **101**, 010504 (2008).

[8] Lukasz Fidkowski, “Entanglement spectrum of topological insulators and superconductors,” *Phys. Rev. Lett.* **104**, 130502 (2010).

[9] Xiao-Liang Qi, Hosho Katsura, and Andreas W. W. Ludwig, “General relationship between the entanglement spectrum and the edge state spectrum of topological quantum states,” *Phys. Rev. Lett.* **108**, 196402 (2012).

[10] Weifei Li, Letian Ding, Rong Yu, Tommaso Roscilde, and

Stephan Haas, “Scaling behavior of entanglement in two- and three-dimensional free-fermion systems,” *Phys. Rev. B* **74**, 073103 (2006).

[11] T. Barthel, M.-C. Chung, and U. Schollwöck, “Entanglement scaling in critical two-dimensional fermionic and bosonic systems,” *Phys. Rev. A* **74**, 022329 (2006).

[12] Michael M. Wolf, “Violation of the entropic area law for fermions,” *Phys. Rev. Lett.* **96**, 010404 (2006).

[13] Dimitri Gioev and Israel Klich, “Entanglement entropy of fermions in any dimension and the widom conjecture,” *Phys. Rev. Lett.* **96**, 100503 (2006).

[14] Brian Swingle, “Entanglement Entropy and the Fermi Surface,” *Phys. Rev. Lett.* **105**, 050502 (2010).

[15] Wenxin Ding, Alexander Seidel, and Kun Yang, “Entanglement entropy of fermi liquids via multidimensional bosonization,” *Phys. Rev. X* **2**, 011012 (2012).

[16] Benoit B Mandelbrot, “The fractal geometry of nature.(w. h. freeman: New york.),” (1983).

[17] Yuval Gefen, Benoit B. Mandelbrot, and Amnon Aharony, “Critical phenomena on fractal lattices,” *Phys. Rev. Lett.* **45**, 855–858 (1980).

[18] Miron Kaufman and Robert B. Griffiths, “Exactly soluble ising models on hierarchical lattices,” *Phys. Rev. B* **24**, 496–498 (1981).

[19] Yuval Gefen, Yigal Meir, Benoit B. Mandelbrot, and Amnon Aharony, “Geometric implementation of hypercubic lattices with noninteger dimensionality by use of low lacunarity fractal lattices,” *Phys. Rev. Lett.* **50**, 145–148 (1983).

[20] Y. Gefen, A. Aharony, and B. B. Mandelbrot, “Phase transitions on fractals. iii. infinitely ramified lattices,” *J. Phys. A: Math. Gen.* **17**, 1277 (1984).

[21] H. Tasaki, “Critical phenomena in fractal spin systems,” *J. Phys. A: Math. Gen.* **20**, 4521 (1987).

[22] Tohru Koma and Hal Tasaki, “Classical XY model in 1.99 dimensions,” *Phys. Rev. Lett.* **74**, 3916–3919 (1995).

[23] Beni Yoshida and Aleksander Kubica, “Quantum criticality from ising model on fractal lattices,” (2014), arxiv:1404.6311 [cond-mat, physics:quant-ph].

[24] Jian Shang, Yongfeng Wang, Min Chen, Jingxin Dai, Xiong Zhou, Julian Kuttner, Gerhard Hilt, Xiang Shao, J. Michael Gottfried, and Kai Wu, “Assembling molecular Sierpiński triangle fractals,” *Nature Chem* **7**, 389–393 (2015).

[25] Chao Li, Xue Zhang, Na Li, Yawei Wang, Jiajia Yang, Gaochen Gu, Yajie Zhang, Shimin Hou, Lianmao Peng, Kai Wu, Damian Nieckarz, Paweł Szabelski, Hao Tang, and Yongfeng Wang, “Construction of Sierpiński Triangles up to the Fifth Order,” *J. Am. Chem. Soc.* **139**, 13749–13753 (2017).

[26] S. N. Kempkes, M. R. Slot, S. E. Freeney, S. J. M. Zevenhuizen, D. Vanmaekelbergh, I. Swart, and C. Morais Smith, “Design and characterization of electrons in a fractal geometry,” *Nat. Phys.* **15**, 127–131 (2019).

[27] Yiping Mo, Ting Chen, Jingxin Dai, Kai Wu, and Dong Wang, “On-Surface Synthesis of Highly Ordered Covalent Sierpiński Triangle Fractals,” *J. Am. Chem. Soc.* **141**, 11378–11382 (2019).

[28] Chen Liu, Yinong Zhou, Guanyong Wang, Yin Yin, Can Li, Haili Huang, Dandan Guan, Yaoyi Li, Shiyong Wang, Hao Zheng, Canhua Liu, Yong Han, James W. Evans, Feng Liu, and Jinfeng Jia, “Sierpinski structure and electronic topology in bi thin films on insb(111)b surfaces,” *Phys. Rev. Lett.* **126**, 176102 (2021).

[29] Edo van Veen, Andrea Tomadin, Marco Polini, Mikhail I. Katsnelson, and Shengjun Yuan, “Optical conductivity of a quantum electron gas in a sierpinski carpet,” *Phys. Rev. B* **96**, 235438 (2017).

[30] Shriya Pai and Abhinav Prem, “Topological states on fractal lattices,” *Phys. Rev. B* **100**, 155135 (2019).

[31] Askar A. Iliasov, Mikhail I. Katsnelson, and Shengjun Yuan, “Hall conductivity of a sierpinski carpet,” *Phys. Rev. B* **101**, 045413 (2020).

[32] Tobias Biesenthal, Lukas J. Maczewsky, Zhaoju Yang, Mark Kremer, Mordechai Segev, Alexander Szameit, and Matthias Heinrich, “Fractal photonic topological insulators,” *Science* **376**, 1114–1119 (2022).

[33] Xiaotian Yang, Weiqing Zhou, Qi Yao, Pengfei Lv, Yunhua Wang, and Shengjun Yuan, “Electronic properties and quantum transport in functionalized graphene sierpinski-carpet fractals,” *Phys. Rev. B* **105**, 205433 (2022).

[34] Sourav Manna, Snehasish Nandy, and Bitan Roy, “Higher-order topological phases on fractal lattices,” *Phys. Rev. B* **105**, L201301 (2022), arxiv:2109.03231 [cond-mat].

[35] Junkai Li, Qingyang Mo, Jian-Hua Jiang, and Zhaoju Yang, “Higher-order topological phase in an acoustic fractal lattice,” *Science Bulletin* **67**, 2040–2044 (2022).

[36] Guanyu Zhu, Tomas Jochym-O’Connor, and Arpit Dua, “Topological order, quantum codes, and quantum computation on fractal geometries,” *PRX Quantum* **3**, 030338 (2022).

[37] Yangang Chen and Guifre Vidal, “Entanglement contour,” *J. Stat. Mech.* **2014**, P10011 (2014).

[38] Ingo Peschel, “Calculation of reduced density matrices from correlation functions,” *J. Phys. Math. Gen.* **36**, L205–L208 (2003).

[39] Israel Klich, “Lower entropy bounds and particle number fluctuations in a fermi sea,” *J. Phys. A: Math. Gen.* **39**, L85–L91 (2006).

[40] Yao Zhou and Peng Ye, “Entanglement signature of hinge arcs, fermi arcs, and crystalline symmetry protection in higher-order weyl semimetals,” *Phys. Rev. B* **107**, 085108 (2023).

[41] R. Rammal and G. Toulouse, “Random walks on fractal structures and percolation clusters,” *J. Physique Lett.* **44**, 13–22 (1983).

[42] Sheldon Goldstein, “Percolation theory and ergodic theory of infinite particle systems,” *IMA Math.* **8**, 121–129 (1987).

[43] Naotaka Kajino, “Spectral asymptotics for laplacians on self-similar sets,” *Journal of Functional Analysis* **258**, 1310–1360 (2010).

[44] Richard F. Bass, Takashi Kumagai, Martin T. Barlow, and Alexander Teplyaev, “Uniqueness of brownian motion on sierpinski carpets,” *J. Eur. Math. Soc.* **12**, 655–701 (2010).

[45] Pok Man Tam, Martin Claassen, and Charles L. Kane, “Topological Multipartite Entanglement in a Fermi Liquid,” *Phys. Rev. X* **12**, 031022 (2022).

[46] Shengjie Zheng, Xianfeng Man, Ze-Lin Kong, Zhi-Kang Lin, Guiju Duan, Ning Chen, Dejie Yu, Jian-Hua Jiang, and Baizhan Xia, “Observation of fractal higher-order topological states in acoustic metamaterials,” *Science Bulletin* **67**, 2069–2075 (2022).

[47] Shengjun Yuan, Hans De Raedt, and Mikhail I. Katsnelson, “Modeling electronic structure and transport properties of graphene with resonant scattering centers,” *Phys. Rev. B* **82**, 115448 (2010).

Supplemental Material

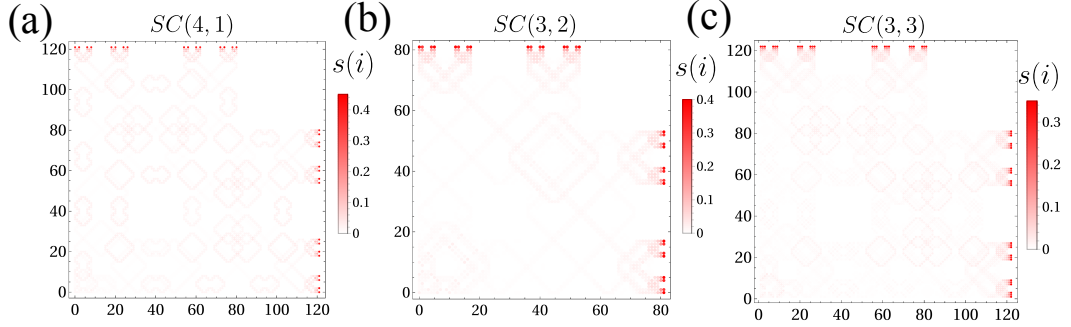


FIG. 6. (a-c) is the EC of the model H_1 on the n th-order approximation $SC(n, s)$ with different unit cell. Here $t = 1$ and $\mu = 0$.

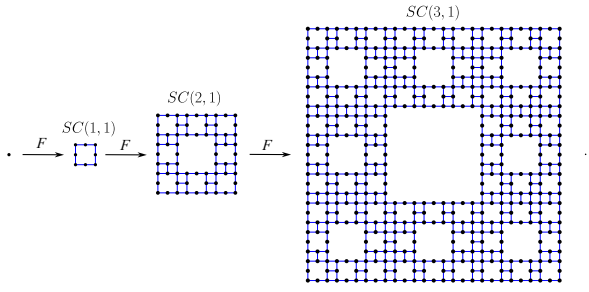


FIG. 7. The illustration of using iteration method F to generate the n th-order approximation $SC(n, 1)$ of Sierpinski carpet with $N = 8^n$ lattice sites.

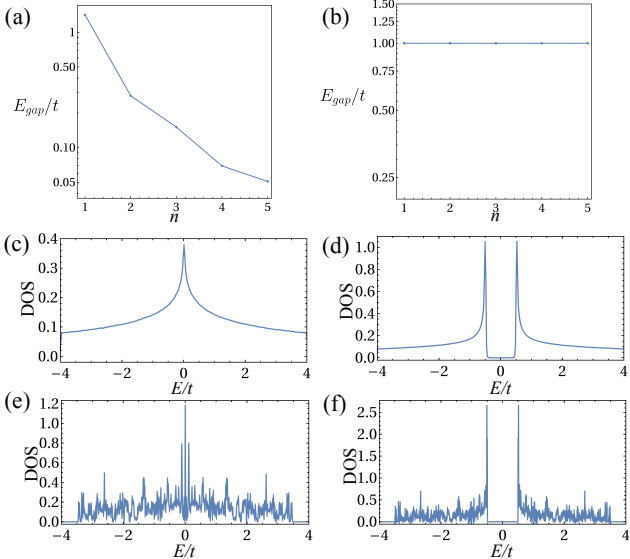


FIG. 8. Scaling of maximum energy gap $\max(E_j)$ for the model and in (a) and (b). (c) and (d) are the DOS of the model and on a square lattice with periodic boundary condition, respectively. (e) and (f) are the DOS of the model and on the approximation $SC(6, 1)$ of Sierpinski carpet, respectively. Here $t = 1$ and $\mu = 0$ in the model, $t = 1, t_1 = 0.5$ in the model.

A. Fractal lattice and Entanglement entropy

Here we discuss how to construct a lattice system with fractal structure. Initially, we consider an initial unit cell U and a fractal iteration method F to generate the fractal lattice. As illustrated in Fig. 7, employing the method F on the cell U iteratively n times allow us to obtain the n th-order approximation $SC(n, s)$ of Sierpinski carpet [16]. Here n represents n th iteration and the number of lattice sites in a unit cell is s^2 . Without loss of generality, when $n \rightarrow \infty$ and setting the lattice constant $l = 1$, the Hausdorff fractal dimension of Sierpinski carpet is defined as $d_f = \lim_{n \rightarrow \infty} \log_{\mathcal{L}} \mathcal{N} = \log_3 8$, where the number of lattice site $\mathcal{N} = s^2 \times 8^n$ in the n th-order approximation $SC(n, s)$ of Sierpinski carpet, and the width of $SC(n, s)$ is $\mathcal{L} = s \times 3^n$. The Hausdorff fractal dimension d_f does not depend on the number s^2 of lattice sites in a unit cell U when $n \rightarrow \infty$. Then, for convenience, we set $s = 1$ in this work.

In free-fermion limit, due to the quadratic form of entanglement Hamiltonian $\mathcal{H}^E = \sum_{i,j} c_i^\dagger h_{i,j}^E c_j$ with $i, j \in A$, then we can unearth the entanglement information from the entanglement Hamiltonian matrix h^E . Meanwhile, the spectrum $\{\varepsilon_\ell\}$ of h^E and the spectrum $\{\xi_\ell\}$ of correlation matrix C^A in the subsystem A have one-to-one correspondence $\varepsilon_\ell = \log[(\xi_\ell)^{-1} - 1]$ with the same eigenvector. For convenience in free-fermion systems, the spectrum $\{\xi_\ell\}$ is usually adopted as entanglement spectrum, and the EE is calculated by the equation $S_A = - \sum_\ell [\xi_\ell \log \xi_\ell + (1 - \xi_\ell) \log(1 - \xi_\ell)]$.

B. Scaling of energy gap and DOS of the model H_1 and H_2 on fractal $SC(n, 1)$

In this part, we discuss the properties of energy spectrum for the models H_1 and H_2 . For the n th-order approximation $SC(n, 1)$ with finite lattice sites, its energy spectrum has a finite number of gaps E_j . Then, we consider the scaling of maximum energy gap $\max(E_j)$ with the number n of iterations increasing. As demonstrated in Fig. 8(a) and (b), we observe that the scaling of $\max(E_j)$ for the model decreases exponentially, while $\max(E_j)$ of the model is invariant.

Furthermore, we consider the density of states (DOS) of

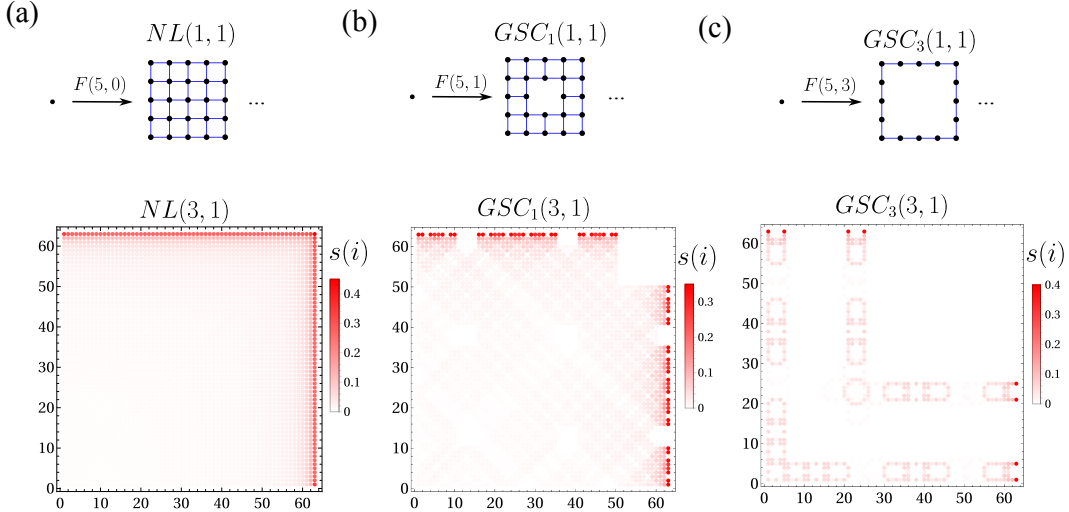


FIG. 9. The upper of (a-c) show the generating process of normal lattice $NL(n, 1)$ and the approximation $GSC_{1(3)}(n, 1)$ generalized Sierpinski carpet. The bottom of (a-c) is the EC of the model H_1 on the normal lattice and the approximation $GSC_{1(3)}(3, 1)$ of generalized Sierpinski carpet. Here $t = 1$ and $\mu = 0$.

the models H_1 and H_2 on $SC(n, 1)$ to provide more information of their energy spectrum. Specifically, when the model H_1 is defined on the square lattice with translation invariance, lattice constant $l = 1$ and periodic boundary condition, we can utilize Bloch band theory to clearly determine its energy spectrum. Moreover, its density of states in thermodynamics limit can be obtained by the energy dispersion $E(\mathbf{k}) = -2t(\cos k_x + \cos k_y) - \mu$ and demonstrated in Fig. 8(c) with $t = 1$ and $\mu = 0$. From the continuity of the DOS in Fig. 8(c), the energy spectrum of the model on square lattice is gapless, and the maximum point of DOS means the nesting Fermi surface appearing.

Next, we consider the model H_1 defined on the n th-order approximation of Sierpinski carpet. To practically determine the energy gap of the the model on $SC(n, 1)$, we adopt the the method in Ref. [47] to calculate its DOS, where the method is very useful and efficient for large lattice system without translation invariance. By using this method, we demonstrated the DOS of the model on the 6th-order approximation $SC(6, 1)$ in Fig. 8(e) for an example, where $SC(6, 1)$ has 8^6 lattice sites. Compared with DOS in Fig. 8(c), we find that although the fractal structure makes the DOS of the model become fluctuated, the DOS is still continuous and its the maximum point is still located at $E = 0$. Meanwhile, by increasing the number n of iterations, the maximum energy gap $\max(E_j)$ of the model on $SC(n, 1)$ becomes more and more small. Therefore, we propose that the model on Sierpinski carpet in thermodynamics limit can be regarded as a gapless system.

Here we consider the DOS of the model H_2 to determine the nature of energy spectrum. Firstly, considering the model H_2 on the square lattice with periodic boundary condition, utilizing Bloch band theory, the DOS of this model in ther-

modynamics limit is determined by the energy dispersion $E(\mathbf{k}) = \pm\sqrt{4t^2(\cos k_x + \cos k_y)^2 + t_1^2}$ and demonstrated in Fig 8(d) with $t = 1$ and $t_1 = 0.5$. Then, we find that the energy spectrum of model in this case has an energy gap. Next, considering the model defined on the approximation $SC(6, 1)$ of Sierpinski carpet as an example, by using the efficient method [47], the energy gap of the model is still existent as shown in Fig. 8(f) with increasing the number n of iteration in $SC(n, 1)$. Meanwhile, compared with the results in Fig. 8(d), the fractal structure of $SC(6, 1)$ induces the fluctuation of the DOS and increases the DOS of maximum point as shown in Fig. 8(f). Meanwhile, by increasing the number n of iterations, the maximum energy gap $\max(E_j)$ of the model H_2 on $SC(n, 1)$ is invariant as shown in Fig. 4 (b). Therefore, we propose that the model on Sierpinski carpet in thermodynamics limit is still a gapped system.

C. More numerical results for EC

For the fractal system, the fractal dimension is determined by the iteration method F and the unit cell U . When the number of iteration $n \rightarrow \infty$, the fractal dimension only depends on the iteration method F . Then, we should study the EC of the model H_1 on the fractal lattice with identical iteration method and different unit cell to show the entanglement fingerprint of fractal geometry. To be specific, in Fig. 6, we demonstrate the numerical results of EC of the model H_1 in three kinds of approximation $SC(n, s)$ of Sierpinski carpet, where the unit cell U has s^2 lattice sites. We observe that for the model H_1 , its EC appears a universal pattern in three kinds of approximation $SC(n, s)$, which is not affected by the unit cell U . Then,

these numerical results show that the structure of EC may only depend on the iteration method.

In the following, we study the effect of iteration method F for the EC of the model H_1 . Firstly, we give a detailed discussion of generalized Sierpinski carpet. As shown in Fig. 9, considering a unit cell with one lattice site, we use an iteration method $F(m, m_f)$ to generate a lattice system, where the system has $m^2 - m_f^2$ unit cells with the width having m unit cells. If $m_f = 0$, then we obtain the normal lattice system $NL(n, 1)$ with trivial fractal structure and fractal dimension $d_f = 2$ in Fig. 9 (a), where n is the number of iteration. When $m_f \neq 0 < m$, then we obtain the the approximation

$GSC_{m_f}(n, 1)$ of generalized Sierpinski carpet with fractal dimension $d_f = \log_m(m^2 - m_f^2)$ in Fig. 9(b) and (d).

Next, we study EC of the model H_1 on the approximation $GSC_{m_f}(n, 1)$ of generalized Sierpinski carpet. To avoid the irrelevant effect for the EC, we choose $n = 3$ to let three lattice systems having identical width as shown in Fig. 9. From the numerical results of EC in the below of Fig. 9(a-c), we find that for the normal lattice $NL(n, 1)$, the EC satisfying the results in Ref. [37] does not have the special pattern. For the generalized Sierpinski carpet, the EC is affected by the iteration method F as shown in Fig. 9(b-c). Then, based on these numerical results, we consider that the EC of the gapless systems with fractal geometry may have a correspondence relation with the iteration method.